

# Range expansion shifts clonal interference patterns in evolving populations

Nikhil Krishnan<sup>1</sup> and Jacob G. Scott<sup>1,2,3</sup>

<sup>1</sup>Case Western Reserve University School of Medicine, Cleveland, OH, 44106, USA

<sup>2</sup>Translational Hematology Oncology Research and Radiation Oncology, Cleveland Clinic, Cleveland OH, 44106, USA

<sup>3</sup>Department of Physics, Case Western Reserve University, Cleveland, OH, 44106, USA

\*npk13@case.edu, scottj10@ccf.org

## ABSTRACT

The movement of a population through space can have profound impacts on its evolution, as observed theoretically, experimentally, and clinically. Furthermore, it has been observed that mutants emerging at the spreading front develop higher frequencies in the population than their counterparts further from the front. Here we use fundamental arguments from population genetics regarding expected time scales of beneficial mutant establishment and fixation in a population undergoing range expansion to characterize the degree of clonal interference expected in various regions while the population is migrating. By quantifying the degree of clonal interference along the wave front of a population undergoing range expansion using a measure we term the ‘Clonal Interference Index’, we show that evolution is increasingly mutation-limited toward the wave tip. In addition, we predict that the degree of clonal interference varies non-monotonically with respect to position along the wave front. The work presented here extends a powerful framework in population genetics to a canonical physical model of range expansion, which we hope allows for continued development of these models in both fields.

## 1 Introduction

2 It has been observed in a variety of clinical and experimental contexts that cell populations in a spatially complex  
3 environment can rapidly adapt to selective pressures, including the presence of antibiotics<sup>1–5</sup>. Theoretical work has  
4 revealed how the spatial dynamics of population movement actively modulate evolutionary dynamics. Indeed, in  
5 many circumstances, movement of a population to a new environment, or range expansion, drives population allele  
6 frequencies from steady state<sup>6</sup>.

7 For example, it has been demonstrated that mutants arising closer to the front of the moving population during  
8 range expansion carry a higher likelihood of fixing throughout the migrating population than in a well-mixed  
9 population<sup>7–9</sup>. Further, range expansion can facilitate fixation of mutants that would otherwise not occur in a static  
10 population<sup>6,10,11</sup>. This can be observed in a canonical reaction-diffusion model of range-expansion (Box 1), which  
11 models population movement in a wave-like manner. In this model, individuals at the front of the wave proliferate  
12 faster than those that do not due to access to empty space<sup>12</sup>. In addition, as the population continues to move,  
13 the offspring of individuals at the wave front remain there and continue to exploit the empty space ahead of the  
14 front. In this way, mutants arising at the wave front have enhanced proliferative capacity. Theoretical work on this  
15 phenomenon, called mutation surfing, often in the context of an analogous stochastic model<sup>13</sup>, has shown that this  
16 phenomenon occurs for deleterious, neutral, and beneficial mutations alike, underscoring the non-trivial impact of  
17 range expansion on evolutionary dynamics<sup>8,14–16</sup>.

18 We hypothesize that the observation that mutation surfing is less likely for a mutant arising from the wave bulk  
19 than a mutant from the wave tip is due to an underlying, characterizable difference in evolutionary regime within  
20 these regions of colonization. Insofar as beneficial mutations arising during range expansion are concerned, previous  
21 work has been limited to the consideration of a wild type population capable of rare acquisition of a single mutation  
22 granting a selective advantage<sup>15,16</sup>.

23 In static populations, however, much of the foundational work in population genetics has provided powerful  
24 frameworks for predicting the dynamics of evolving populations bearing multiple beneficial mutations<sup>17,18</sup>. In such  
25 populations, the dependence of the fate of beneficial mutants on population and selection characteristics has been  
26 well described<sup>19–21</sup>. Beyond the limits of these models’ constraints and their predictive power, this work has had  
27 profound influence on our modern conceptualization and intuition about evolution. Here we seek to characterize  
28 the evolutionary regimes experienced by a population undergoing range expansion that acquires multiple beneficial

29 mutation and displays clonal interference, or interactions between mutants while they fix. We achieve this by  
 30 considering a stochastic Fisher wave with mutation describing such a population. We then quantify the likelihood  
 31 of clonal interference by applying classical arguments regarding the population dynamics of beneficial mutations  
 32 within the sub-population at each position using our Clonal Interference Index. Ultimately, we seek to build a global  
 33 picture of evolutionary regime and the resulting clonal interference over range expansion space.

### Box 1: Range Expansion Dynamics

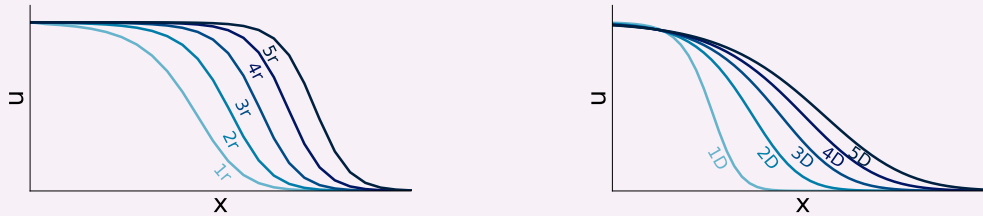
#### Fisher equation: 1D reaction-diffusion

$$\partial_t u = D\partial_x^2 u + ru(1-u) \quad (1)$$

where,

- $u(x, t)$  is the density of traveling particles as a function of position,  $x$  and time,  $t$
- $D$  is the diffusion constant
- $r$  is the reaction rate

and at a given time  $r$  and  $D$  alter the wave profile in the following way respectively:



34

## Results

35  
 36 We begin by considering a deterministic description for reaction-diffusion of a bacterial population in one dimension  
 37 (Box 1). Given an average growth rate of  $r$  and a maximum diffusion constant  $D_0$ , we find that the maximum distance  
 38 diffused within a generation is  $\sqrt{D_0/r}$ . We rescale position  $x$  by this distance to define a dimensionless position  
 39 variable  $\tilde{x} = x\sqrt{r/D_0}$ . Population density  $b(x, t)$  is scaled by its carrying capacity  $K$ :  $\tilde{b} = b/K$ , and the diffusion  
 40 constant  $D$  by  $D_0$ , the maximum diffusion constant:  $\tilde{D} = D/D_0$ <sup>22</sup>. Hereafter, we refer to these dimensionless  
 41 parameters and variables without the tildes for notational convenience. We thus obtain the familiar Fisher's equation:  
 42  $\partial_t b = D\partial_x^2 b + b(1-b)$  for change in population density with respect to time and position. With this description of  
 43 range expansion we can introduce a beneficial mutation that arises with rate  $U_b$  and selective advantage  $\alpha \equiv r_m/r_w$ ,  
 44 where  $r_w$  is the average wild-type growth rate and  $r_m$  is the average mutant growth rate. Noting that at early times  
 45 in a mutant's life and at small population sizes stochastic effects dominate, we have spatio-temporal dynamics for  
 46 the wild-type ( $b$ ) and mutant ( $b_m$ ):

$$\partial_t b = D\partial_x^2 b + r_w b(1 - (b + b_m)) - bU_b + \sqrt{\gamma_b(b)b(1 - (b + b_m))}\eta(x, t), \text{ and} \quad (2)$$

$$\partial_t b_m = D\partial_x^2 b_m + r_m b_m(1 - (b + b_m)) + bU_b + \sqrt{\gamma_{b_m}(b_m)b_m(1 - (b + b_m))}\eta_m(x, t). \quad (3)$$

47 where  $\eta(x, t)$  and  $\eta_m(x, t)$  are Itô white noises satisfying  $\langle \eta(x_1, t_1)\eta(x_2, t_2) \rangle = \delta(t_1 - t_2)\delta(x_1 - x_2)$ , and  $\gamma_b(b)$  and  
 48  $\gamma_{b_m}(b_m)$  describe the magnitude of fluctuations for the wild-type and mutant waves respectively. It can be shown that  
 49  $\gamma_b(b)$  and  $\gamma_{b_m}(b_m)$  are determined by the sum of variance of birth and non-birth events divided by their co-variance  
 50 for the wild-type and mutant populations respectively<sup>23-27</sup>. In other words, the strength of these fluctuations varies  
 51 indirectly with population size,  $N$ , thus adding stochastic genetic drift effects to the deterministic Fisher equation.  
 52 In this way, the choice of  $N$ , which depends on  $K$ , essentially determines the minimum density which is 'counted' in  
 53 our simulations and gives compact support  $[1/N, 1]$  in  $b$  and  $b_m$ . We will discuss the impact of this choice on the  
 54 predicted fate of a beneficial mutant later.

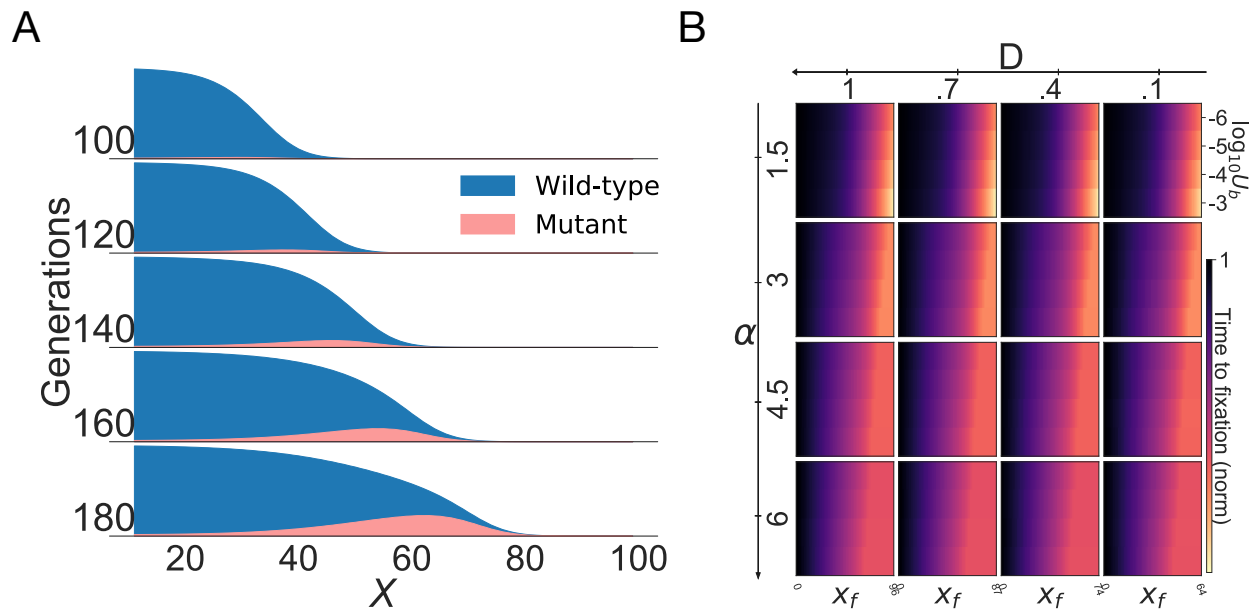


**Figure 1. A: Balance between mutational supply and influence of genetic drift determines local mutant density.** Wave profile during diffusive range expansion at various time points. Mutation rate  $U_b = 10^{-3}$ , selective advantage  $\alpha = 1.5$ , and diffusion constant  $D = 0.4$ . **B: Higher selective advantage and beneficial mutation rate decrease relative local fixation time toward the wave tip.** Simulated time to ‘local’ mutant fixation by position along wave front,  $x_f$ , over a range of mutation rates  $U_b$ , selective advantage  $\alpha$ , and diffusion coefficients  $D$

Simulation of equation (2) was initialized with a ‘Gaussian packet’ of wild-type cells of the form  $\exp(-x^2/\sigma^2)$  where  $\sigma$ , which we set to 2, determines the shape of this packet<sup>22</sup>. We additionally set  $r_w = 0.1$  and  $N = 1 \times 10^7$ . Simulating this one mutant reaction-diffusion system forward through time using an Euler-Maruyama scheme (Figure 1) reveals that at a given time before fixation throughout the wave front, the highest mutant frequency is seen at the very wave tip, while the highest absolute density is seen at a position further away from the tip, with diminishing mutant density behind this point. This pattern likely reflects the balance between mutational supply of a larger population away from the wave tip and enhanced stochastic effects toward the wave tip<sup>8</sup>.

We additionally measured the time for ‘local fixation’ at each position along the wave front. The wave front was defined by the initial wild-type wave profile which remains unchanged in the frame of reference traveling at the average velocity of the wave in the absence of mutants. Here, we introduce the concept of a ‘deme’, by which we examine a subpopulation of the wave along a length. In this way we conceptualize the cell in the context of Equations (2), (3), as a discrete number of individuals.

The number of individuals that define a deme of length  $L \ll 1$  centered at a given position  $x$  with carrying capacity  $K$  as before is then  $N = K \int_{x-L/2}^{x+L/2} b(x') dx'$ . The average initial wave front profile,  $b_i(x)$ , then satisfies the following equation:

$$0 = D\partial_x^2 b_i + b_i r_w (1 - b_i) + v\partial_x b_i, \quad (4)$$

and is defined for all  $x$  where

$$K \int_{x-L/2}^{x+L/2} b(x') dx' > 1, \quad (5)$$

and otherwise is 0. The length of the wave front,  $L_f$ , is then defined by the maximum  $x$  for which  $b_i$  is defined as in Equations (4), (5).  $v$  is the average velocity of the wave front ( $2\sqrt{Dr_w}$ ), as in the classic result for a Fisher (Kolmogorov–Petrovsky–Piskunov) wave. At any subsequent time after the initial wave profile has evolved, we

74 examine the wild-type wave front, recording the local fixation time as the time at which  $K \int_{x_f-L/2}^{x_f+L/2} b(x'_f) dx'_f < 1$ ,  
75 for every integer  $x_f \leq L_f$  where  $x_f$  is position in the frame of reference travelling at the average velocity of the  
76 initial wave front:  $x_f = x - vt$  with  $v$  as above.

77 Predictably, increasing  $\alpha$  and  $U_b$  causes mutations to reach local fixation in fewer generations along the entire  
78 wave front (1B). By normalizing to the time to fixation at the beginning of the wave front we see that the *difference*  
79 between the time to local fixation at the beginning at the wave front and at the wave tip is also increased with higher  
80 selective advantage and mutation rate. The results here directly mirror the trend in mutant surfing probabilities  
81 with respect to position shown by Lehe *et al.*<sup>15</sup>. Assuming mutants that fix throughout the population first take  
82 over and surf at the wave front, local fixation at the wave tip earlier in time before regions further from the wave tip  
83 as we observe in Figure 1 is a consequence of the increased mutant surfing probability near the tip of the expanding  
84 population as previously established<sup>15</sup>.

85 However, as a single mutant population arises and survives long enough to surf along the front and eventually fix  
86 throughout the front, subsequent mutational events may contribute to fixation of the mutant population. While Lehe  
87 *et al.* phenomenologically correct for this when computing surfing probability with respect to position, assuming  
88 it occurs rarely, the degree of this effect at various parameters and positions in the population undergoing range  
89 expansion was not discussed.

90 While there has been limited description of beneficial mutants competing as they fix in a spatial context via game  
91 theoretical models, the growth dynamics of such a population undergoing range expansion are poorly understood  
92 [18, 28–30](#).

93 Though an analytic description of fixation times allowing for clonal interference is difficult even in a well-mixed  
94 population, we can assess under what conditions and at what positions along the wave profile these considerations are  
95 non-trivial. In the case of a well-mixed population, classic analysis has lended a framework by which to qualitatively  
96 classify the extent of clonal interference in a well mixed-population (Box 2). Briefly one can derive an expression  
97 for the average fixation time of a beneficial mutant that has not gone extinct and does not interact with another  
98 growing clonal population,  $\langle \tau_{fix} \rangle$ . This is compared to the average expected time for a mutant that is destined to  
99 eventually fix to arise in the population, or the average establishment time  $\langle \tau_{est} \rangle$ <sup>17</sup>.

100 When the average fixation time is far shorter than the average time for such a mutant to be established, the  
101 population can be approximated as being isogenic with the fittest genotype available, termed strong selection weak  
102 mutation (SSWM)<sup>17, 20</sup>. When the aforementioned average fixation and establishment times become comparable,  
103 separate mutant clonal populations will likely exist simultaneously, and compete with each other as the separate  
104 clonal lineages grow<sup>18</sup>. The relative contributions of mutation rate and mutant fitness benefit underlying this behavior  
105 is sometimes termed strong selection strong mutation (SSSM). As the establishment time becomes increasingly  
106 short relative to fixation time, weak selection strong mutation (WSSM) takes places and many clonal populations  
107 are expected to coexist at a time. As described in Box 2,  $\langle \tau_{est} \rangle$  and  $\langle \tau_{fix} \rangle$  are determined by  $N$ ,  $U_b$ , and  $s$ ,  
108 and the constraints on the above regimes can be stated in terms of these parameters, as is commonly seen in the  
109 literature<sup>17, 18, 20, 31</sup>.

110 While these regimes are theoretical simplifications, evidence indicates they each serve to simplify biologically  
111 observable behavior<sup>32–34</sup>. In kind, we can comment on the evolutionary regime of the local environment during  
112 range expansion by a similar comparison of fixation and establishment times.

113 To find the expected establishment time,  $\langle \tau_{est} \rangle$  of mutants with respect to position we must calculate the survival  
114 probability of a single mutant arising at each position. We achieve this by assuming the survival probability,  $u(x)$ ,  
115 satisfies a backward Kolmogorov equation,

$$0 = \partial_x^2 u + ur_m(1 - b_i) - v\partial_x u - u^2, \quad (6)$$

## Box 2: Population Genetics

### Beneficial mutations in a well-mixed population :

For a large asexual population with fixed size  $N$ , and finite alleles conferring fitness advantage  $s$ , mutated between at rate  $U_b$ .

The average time for a single mutant that does not go extinct to fix on average,  $\langle\tau_{fix}\rangle$ , is:

$$\langle\tau_{fix}\rangle \approx \frac{1}{s} \log(Ns).$$

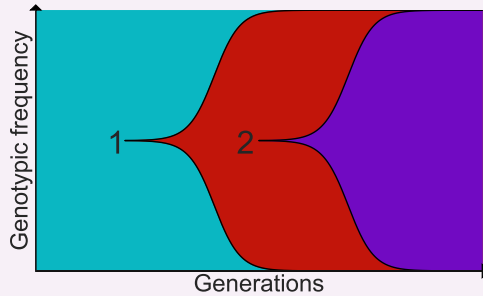
The average time for a mutant to arise and survive,  $\langle\tau_{est}\rangle$ , is

$$\langle\tau_{est}\rangle \approx 1/NU_b s.$$

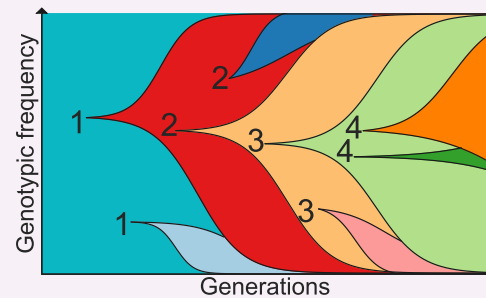
### Dynamical regimes of beneficial mutations:

When  $\langle\tau_{est}\rangle \gg \langle\tau_{fix}\rangle$  beneficial mutations fix ‘one at a time’ and at  $t \geq \tau_{fix}$  the population is (on average) isogenic.

When mutants arise frequently enough relative to the fixation time to interfere with each other, or  $\langle\tau_{est}\rangle < \langle\tau_{fix}\rangle$ .



This regime is also known as the strong selection weak mutation (SSWM) regime, to highlight the *relative* strength of selection and mutation compared to each and other and  $N$ .



When  $\langle\tau_{fix}\rangle$  is sufficiently larger than  $\langle\tau_{est}\rangle$ , the population is expected to always be polygenic, often termed the weak selection, strong mutation (WSSM) regime. When they are comparable, clones experience competition as they fix, termed strong selection strong mutation (SSSM)<sup>17, 18, 31</sup>.

116

and saturates at  $\sim r_m$  in the far reaches of the wave tip

117

Equations of the same form as Equation (6) classically have been used to describe a branching random walk<sup>15, 21</sup>.

118

That it describes the survival probability of single beneficial mutant as a function of position is discussed further in the Methods section.

119

We use Equation (6) to estimate the average establishment time,  $\langle\tau_{est}\rangle$ , of a mutant with respect to position along wave front  $x_f$  as before. Given that mutants appear in the population at average rate  $U_b$ ,

120

121

$$\langle\tau_{est}\rangle \approx KU_b \int_{x_f - L/2}^{x_f + L/2} b(x'_f) u(x'_f) dx'_f \quad (7)$$

122

at a given  $x_f$ .

123

To find the average ‘local’ fixation time of a mutant that does not go extinct, we turn our attention again to the wave front. A mutant arising in the wave front that does not go extinct will fix within its deme by diffusing from its initial position in the frame of the wild-type wave to the wave tip where there are no wild-type individuals within its deme, a distance  $L_f - x_f$ . It will then fix at  $x_f$  where it arose by surpassing the wild type wave front by an additional distance  $L_f - x_f$  (See Methods). We thus obtain:

124

125

126

127

128

129

$$\langle\tau_{fix}\rangle \approx \frac{L_f - x_f}{\sqrt{D}(\sqrt{r_m} - \sqrt{r_w})}. \quad (8)$$

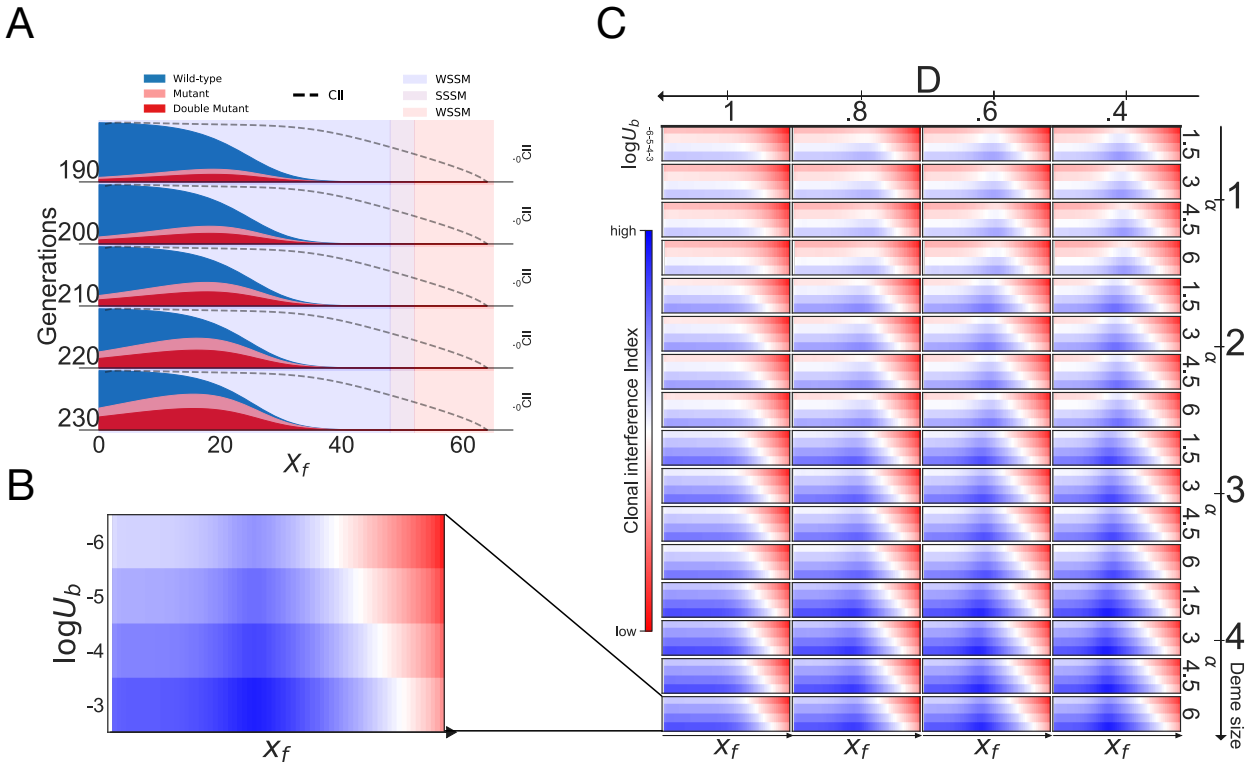


**Figure 2. A: Clonal Interference Index predicts concurrent mutant and double mutant populations in wave bulk.** Wave front of spreading population wave acquiring beneficial mutations at discrete time points with calculated Clonal Interference Index at each position,  $x_f$  on wave front. **B: The wave tip is less likely to display clonal interference.** CII at each position along wave front with varying  $U_b$ . **C: Smaller deme sizes and mutation rate decrease likelihood of observing clonal interference at a given position.** CII along wave front over a range of  $U_b$ ,  $\alpha$ , and  $D$  as we varied relative deme size.

130 To quantify the eco-evolutionary regime defined by the relative fixation and establishment times of a beneficial  
 131 mutant at a given location we define the Clonal Interference Index (CII):

$$CII := \log(\tau_{fix}/\tau_{est}), \quad (9)$$

132 as calculated from Equations (6) - (8). Accordingly  $CII > 0$  indicates that clonal interference is expected, and  
 133  $CII \ll 0$ , indicates that clonal interference is unlikely.

134 We evaluate the concordance of CII to simulated range expansion as before by simulating equations (2) and  
 135 (3), but modified to allow for the development of up to five mutations, each with an identical additional selective  
 136 advantage ( $\alpha$ ) compared to the clone with one less mutation following Desai *et al.*<sup>17</sup>. For the initial wave profile of  
 137 the simulated wave satisfying Equations (4) - (5) as before, Equation (6) is numerically solved to find the  $\langle \tau_{est} \rangle$  with  
 138 Equation (7) at each position along the initial wild type wave profile. In addition  $\langle \tau_{fix} \rangle$  for a mutant arising at  $x_f$   
 139 is calculated from Equation (8). Again, we note that these calculations be performed with varying deme size, which  
 140 impacts  $\langle \tau_{fix} \rangle$  by altering the length of the the wave front, and  $\langle \tau_{fix} \rangle$  by altering the mutational supply available in  
 141 each deme.

142 For a given wave profile, a deme size can be chosen such that the CII reflects a transition between eco-evolutionary  
 143 regime along the wave profile relevant at times on the order of  $\langle \tau_{fix} \rangle$  (Figure 2). Indeed, the appropriate choice of  
 144 deme size for a given analysis depends on the specific question being asked, but as seen in Figure 2, this choice impacts  
 145 the CII in intuitive ways. In general, the smaller the deme size, the faster the time for local fixation and the longer

146 the time for mutant establishment, resulting in a lower likelihood of clonal interference within a deme. Additionally,  
147 model mutation rate predictably alters clonal interference index at a given deme size (Figure 2C). Specifically, with  
148 a given (sufficiently high)  $\alpha$ , the lower the  $U_b$ , the larger the portion of the wave with a low CII corresponding to  
149 the SSWM regime. As a result of the structure of the expression used to estimate average establishment time,  $x_f$   
150 with maximum CII is  $0 < x_f < L_f$ <sup>17</sup>. Subsequently, we predict clonal interference is maximized at some position  
151 between between the onset of the wave front and wave tip. This reflects the optimization of surfing probability and  
152 population density  $b(x_f)u(x_f)$  in Equation (9)<sup>15</sup>.

153 That CII is generally lower toward the front of the wave for a given deme size suggests that the same local  
154 eco-evolutionary characteristics at the wave tip that yield the increased global fixation probabilities previously  
155 observed give rise to mutation-limited dynamics when multiple mutations are allowed to occur<sup>1,15</sup>. In accordance  
156 with this observation, the eco-evolutionary dynamics that cause mutant fixation probability to decay away from the  
157 tip give rise to increased clonal interference (Figure 2B).

## 158 Discussion

159 Our analysis shows how the relative balance of expected fixation and establishment times for a single mutant  
160 arising from within a population undergoing range expansion modulate the extent of clonal interference expected  
161 as a function of position. We show this by connecting canonical reaction-diffusion models of range expansion in  
162 a population governed by accepted equations from population genetics capable of multiple beneficial mutations  
163 which we assume to be of equal selective advantage. We present a clonal interference index as a way to quantify  
164 the predicted clonal interference at each position as determined by a comparison of average local mutant fixation  
165 and establishment times. Our results show that the evolutionary dynamics approach a mutation-limited regime  
166 toward the wave tip during range expansion, and that clonal interference is maximized between the wave tip and the  
167 onset of the wave front. In characterizing the local clonal interference likelihood of the population during range  
168 expansion we learn about an essential influence on its evolutionary dynamics that persist if range expansion was no  
169 longer occurring or took on a more complex form, such as reaction-diffusion-advection. In this way we present a  
170 generalizable framework at the confluence of mathematical biology and population genetics allowing for analysis of  
171 evolutionary regimes during range expansion.

## 172 Methods

### 173 Mutant fixing probability

As in the heuristic analysis of Lehe *et al.*, we begin by considering that the average wild-type wave front  $b(x_f)$ , in  
the absence of mutants, which is stable through time.  $x_f$  is position in the frame of the wave front with velocity  
 $v$ :  $x_f = x - vt$ . From Equation (3) the average mutant density  $\langle b_m(x_f, t) \rangle$  while the mutant population makes a  
negligible contribution toward carrying capacity is as follows:

$$\partial_t b_m = D \partial_{x_f}^2 b_m + r_m b_m (1 - b). \quad (10)$$

174 If we imagine a mutant at time  $t$  and position  $x_f$ , the probability  $\rho(x_f, t | X_f, T)$  of finding the mutant at some  
175 short time later,  $T$  and some slightly different position  $X_f$  can be substituted into Equation (10) by assuming  
176  $\rho(x_f, t | X_f, T) \approx \langle b_m(x_f, t) \rangle$ ,

$$\partial_t \rho = D \partial_{x_f}^2 \rho + r_m \rho (1 - b). \quad (11)$$

177 To find the probability of fixation  $u(x_f)$  for a mutant arising from  $X_f$  we note the following:

$$u(X_f) = \int_{-\infty}^{\infty} \rho(x_f, t | X_f, T) u(x) dx, \quad (12)$$

178 as  $u$  essentially denotes the survival probability after a long time. Substituting Equation (11) into the time derivative  
179 of (12), and integrating we obtain:

$$0 = \partial_x^2 u + u r_m (1 - b_i) - v \partial_x u. \quad (13)$$

180 Following Lehe *et al.*, we apply a  $u^2$  correction term to obtain Equation (6) which yields a saturation of the  
181 mutant probability at  $r_m$  in the critical branching process limit. This heuristic analysis is a useful intuitive framework  
182 for the mutant fixation probability and more formally approximates the fixation probability as a solution of a  
183 continuous backward Kolmogorov equation, the derivation of which can be found in standard texts, and has been  
184 previously applied for approximating mutant surfing probabilities<sup>8,15</sup>.

### 185 Mutant fixation time

186 For the wild type wave profile in the moving frame, we note that a mutant arising in the wave front takes over the  
187 population upon surviving long enough to outpace the wild type wave front. Conditional on this survival, we note  
188 that for a wave front of constant length  $L_f$  defined as in the Results section and mutant arising at  $x_f$ , the difference  
189  $L_f - x_f$  is the distance the mutant must travel along the wave front where the wild-type population is decayed  
190 below 1 and the mutant population has fixed within its deme.

191 In the frame of the wave front, ‘local’ fixation is defined as occurring when the mutant fixes at the position  $x_f$   
192 where it arose. This occurs once the mutant outpaces the wild type wave front and travels an additional distance  
193  $L_f - x_f$  in the wild type frame, so that  $x_f$  is occupied by the fixing mutant front, and the wild type front has  
194 now decayed below 1 here as well. Given the fixing mutant in the moving frame as velocity  $v_{m_f}$  and must travel a  
195 distance  $2(L_f - x_f)$ , we find

$$\langle \tau_{fix} \rangle \approx 2 \frac{L_f - x_f}{v_{m_f}}. \quad (14)$$

196 We note the deterministic velocity of the mutant wave front in the frame traveling  $v_{m_f}$  is

$$v_{m_f} = 2(\sqrt{Dr_m} - \sqrt{Dr_w}), \quad (15)$$

197 from the average deterministic velocity of a Fisher wave. Thus, we obtain Equation (7),

$$\langle \tau_{fix} \rangle \approx \frac{L_f - x_f}{\sqrt{D}(\sqrt{r_m} - \sqrt{r_w})}.$$

## 198 References

- 199 1. Comins, H., Hassell, M. & May, R. The spatial dynamics of host–parasitoid systems. *J. Animal Ecol.* 735–748  
200 (1992).
- 201 2. Markussen, T. *et al.* Environmental heterogeneity drives within-host diversification and evolution of *Pseudomonas*  
202 *aeruginosa*. *MBio* 5, e01592–14 (2014).
- 203 3. Ciofu, O. & Tolker-Nielsen, T. Tolerance and resistance of *Pseudomonas aeruginosa* biofilms to antimicrobial  
204 agents—how *P. aeruginosa* can escape antibiotics. *Front. microbiology* 10, 913 (2019).
- 205 4. Fusco, D., Gralka, M., Kayser, J., Anderson, A. & Hallatschek, O. Excess of mutational jackpot events in  
206 expanding populations revealed by spatial Luria–delbrück experiments. *Nat. communications* 7, 12760 (2016).
- 207 5. Baym, M. *et al.* Spatiotemporal microbial evolution on antibiotic landscapes. *Science* 353, 1147–1151 (2016).
- 208 6. Excoffier, L., Foll, M. & Petit, R. J. Genetic consequences of range expansions. *Annu. Rev. Ecol. Evol. Syst.* 40,  
209 481–501 (2009).
- 210 7. Hallatschek, O., Hersen, P., Ramanathan, S. & Nelson, D. R. Genetic drift at expanding frontiers promotes  
211 gene segregation. *Proc. Natl. Acad. Sci.* 104, 19926–19930 (2007).
- 212 8. Hallatschek, O. & Nelson, D. R. Gene surfing in expanding populations. *Theor. population biology* 73, 158–170  
213 (2008).
- 214 9. Klopstein, S., Currat, M. & Excoffier, L. The fate of mutations surfing on the wave of a range expansion. *Mol.*  
215 *biology evolution* 23, 482–490 (2005).
- 216 10. Edmonds, C. A., Lillie, A. S. & Cavalli-Sforza, L. L. Mutations arising in the wave front of an expanding  
217 population. *Proc. Natl. Acad. Sci.* 101, 975–979 (2004).



- 218 **11.** Burton, O. & Travis, J. Landscape structure and boundary effects determine the fate of mutations occurring  
219 during range expansions. *Heredity* **101**, 329 (2008).
- 220 **12.** Fisher, R. A. The wave of advance of advantageous genes. *Annals eugenics* **7**, 355–369 (1937).
- 221 **13.** Kimura, M. & Weiss, G. H. The stepping stone model of population structure and the decrease of genetic  
222 correlation with distance. *Genetics* **49**, 561 (1964).
- 223 **14.** Travis, J. M. *et al.* Deleterious mutations can surf to high densities on the wave front of an expanding population.  
224 *Mol. biology evolution* **24**, 2334–2343 (2007).
- 225 **15.** Lehe, R., Hallatschek, O. & Peliti, L. The rate of beneficial mutations surfing on the wave of a range expansion.  
226 *PLoS computational biology* **8**, e1002447 (2012).
- 227 **16.** Farrell, F. D., Gralka, M., Hallatschek, O. & Waclaw, B. Mechanical interactions in bacterial colonies and the  
228 surfing probability of beneficial mutations. *J. The Royal Soc. Interface* **14**, 20170073 (2017).
- 229 **17.** Desai, M. M. & Fisher, D. S. Beneficial mutation–selection balance and the effect of linkage on positive selection.  
230 *Genetics* **176**, 1759–1798 (2007).
- 231 **18.** Sniegowski, P. D. & Gerrish, P. J. Beneficial mutations and the dynamics of adaptation in asexual populations.  
232 *Philos. Transactions Royal Soc. B: Biol. Sci.* **365**, 1255–1263 (2010).
- 233 **19.** Haldane, J. B. S. A mathematical theory of natural and artificial selection, part v: selection and mutation. **23**,  
234 838–844 (1927).
- 235 **20.** Gillespie, J. H. Molecular evolution over the mutational landscape. *Evolution* **38**, 1116–1129 (1984).
- 236 **21.** Kimura, M. & Ohta, T. Probability of gene fixation in an expanding finite population. *Proc. Natl. Acad. Sci.*  
237 **71**, 3377–3379 (1974).
- 238 **22.** Croze, O. A., Ferguson, G. P., Cates, M. E. & Poon, W. C. Migration of chemotactic bacteria in soft agar: role  
239 of gel concentration. *Biophys. journal* **101**, 525–534 (2011).
- 240 **23.** Doering, C. R., Mueller, C. & Smereka, P. Interacting particles, the stochastic fisher–kolmogorov–petrovsky–  
241 piscounov equation, and duality. *Phys. A: Stat. Mech. its Appl.* **325**, 243–259 (2003).
- 242 **24.** Hallatschek, O. & Korolev, K. Fisher waves in the strong noise limit. *Phys. review letters* **103**, 108103 (2009).
- 243 **25.** Birzu, G., Hallatschek, O. & Korolev, K. S. Fluctuations uncover a distinct class of traveling waves. *Proc. Natl.*  
244 *Acad. Sci.* **115**, E3645–E3654 (2018).
- 245 **26.** Gandhi, S. R., Yurtsev, E. A., Korolev, K. S. & Gore, J. Range expansions transition from pulled to pushed  
246 waves as growth becomes more cooperative in an experimental microbial population. *Proc. Natl. Acad. Sci.*  
247 **113**, 6922–6927 (2016).
- 248 **27.** Birzu, G., Matin, S., Hallatschek, O. & Korolev, K. S. Genetic drift in range expansions is very sensitive to  
249 density feedback in dispersal and growth. *arXiv preprint arXiv:1903.11627* (2019).
- 250 **28.** Gerrish, P. J. & Lenski, R. E. The fate of competing beneficial mutations in an asexual population. *Genetica*  
251 **102**, 127 (1998).
- 252 **29.** Kaznatcheev, A., Scott, J. G. & Basanta, D. Edge effects in game-theoretic dynamics of spatially structured  
253 tumours. *J. The Royal Soc. Interface* **12**, 20150154 (2015).
- 254 **30.** Kaznatcheev, A., Peacock, J., Basanta, D., Marusyk, A. & Scott, J. G. Fibroblasts and alectinib switch the  
255 evolutionary games played by non-small cell lung cancer. *Nat. ecology & evolution* **3**, 450 (2019).
- 256 **31.** Gillespie, J. H. Some properties of finite populations experiencing strong selection and weak mutation. *The Am.*  
257 *Nat.* **121**, 691–708 (1983).
- 258 **32.** Joseph, S. B. & Hall, D. W. Spontaneous mutations in diploid *saccharomyces cerevisiae*: more beneficial than  
259 expected. *Genetics* **168**, 1817–1825 (2004).
- 260 **33.** Drake, J. W. Avoiding dangerous missense: thermophiles display especially low mutation rates. *PLoS genetics*  
261 **5**, e1000520 (2009).
- 262 **34.** Hao, D., Wang, L. & Di, L.-j. Distinct mutation accumulation rates among tissues determine the variation in  
263 cancer risk. *Sci. reports* **6**, 19458 (2016).

## 264 **Acknowledgements**

265 The authors would like to thank Dr. Diana Fusco for her thoughtful feedback and discussion. JGS would like to  
266 thank the NIH Loan Repayment Program for their generous support and the Paul Calabresi Career Development  
267 Award for Clinical Oncology (NIH K12CA076917).

## 268 **Author contributions statement**

269 NK performed the mathematical analysis, wrote the code, performed the simulations, analyzed the data and wrote  
270 the manuscript. JGS analyzed the data and wrote the manuscript.

## 271 **Code availability**

272 The code to perform the numerical simulations is available via github at [https://github.com/nkrishnan94/](https://github.com/nkrishnan94/Range-Expansion-Eco-Evo-Regime)  
273 [Range-Expansion-Eco-Evo-Regime](https://github.com/nkrishnan94/Range-Expansion-Eco-Evo-Regime).